# Predicted and Measured Antenna Patterns of the European Large Deployable Reflector

C. Cappellin [(1)], M. Lori [(2)], A. Geise [(3)], C. Hunscher [(3)], L. Datashvili [(4)]
[1] TICRA: Copenhagen, Denmark, cc@ticra.com
[2] HPS: Munich, Germany, Lori@hps-gmbh.com
[3] Airbus Defence & Space: Ottobrunn, Germany, alexander.geise@airbus.com, christian.hunscher@airbus.com
[4] LSS: Garching, Germany, leri.datashvili@largespace.de

***Abstract*—The European Large Deployable Reflector (LDR) antenna underwent RF test in November 2020, becoming the first 5.1 m antenna in light mesh technology developed and measured in Europe. In this paper we present the correlation between the measured and predicted antenna patterns at 10.65 GHz.**

***Index Terms*—RF performances, RF predictions, RF measurements.**

## I. INTRODUCTION

Large deployable reflectors are of vital importance for future telecommunication, Earth observation and science missions, where enhanced footprint and resolution are required and ensured by electrically very large reflector antenna sizes. One such example is the Copernicus Imaging Microwave Radiometer (CIMR) mission currently undergoing phase B2 studies. The CIMR instrument is a state-of-the-art conical scanning radiometer made by a deployable reflector of 8 meter projected aperture diameter, which will measure sea-surface temperature, sea-ice concentration and sea-surface salinity with unprecedented accuracy and spatial resolution from L to Ka band.

LDRs have existed in the US for more than three decades, see [1][2], giving rise to numerous successful launches. To enhance the Technology Readiness Level (TRL) of European LDRs and allow technology independence in space, the European Commission decided to complement the development financed in the last decade by the European Space Agency, and thus co-funded the Large European Antenna (LEA) project within the Horizon 2020 framework from 2017 to 2021, [3]. Under the lead of HPS GmbH, a consortium of 15 companies from six European countries won the LEA project and designed, analysed, manufactured and assembled a protoflight model (PFM) of a 5.1 meters deployable reflector antenna in light mesh technology. TICRA, LSS and Airbus in Ottobrunn were part of the consortium.

The LEA antenna is an offset parabolic reflector with f/D equal to 1 realized by two tension nets kept together by tension ties, an RF reflecting lightweight tricot mesh attached to the front tension net, and a deployable truss [4]. The front tension net determines the shape of the reflector, while the lightweight tricot mesh determines its reflectivity. The tension nets are constituted by triangular facets with an average facet size of 327 mm, producing grating lobes at well-defined positions in the far field, [5].

The RF measurement of the LDR antenna was performed in X band (10.65 GHz) using Airbus' Portable Antenna Measurement System (PAMS) [6], in Ottobrunn, Germany. PAMS provides the probe corrected far-field pattern obtained from the radiated near-field, sampled on an arbitrary acquisition surface by a crane-based gondola probe. The RF measurement of the LEA antenna was the first test of the qualification campaign needed to certify TRL 8 of the PFM during 2021. TICRA had the task of providing RF simulations of the LDR antenna performance throughout the LEA project and comparing them with the measured results.

The purpose of the present paper is to show the results of the correlation between the measured and predicted antenna patterns of the LEA antenna. In particular, Section II describes the RF model developed by TICRA, while Section III focuses on the comparison between RF measurements and predictions. Conclusions are finally drawn in Section IV.

## II. RF MODEL

The LEA antenna underwent RF test according to schedule in November 2020, despite the worldwide challenges due to COVID-19. A picture of the LEA antenna in the RF test facility in Ottobrunn is shown in Fig. 1.

TICRA had the task to provide RF predictions of the LEA antenna as installed in the Airbus RF test chamber. The RF predictions were based on a detailed RF model of the LEA reflector and deployable truss, reflective tricot mesh and feed system in the GRASP and ESTEAM software within TICRA Tools, [7]. The RF model of the LEA antenna in the Airbus RF test chamber developed by TICRA is shown in Fig. 2 and consists of:

1. A reflector antenna with measured surface provided by HPS, designed rim provided by LSS and tricot mesh with dielectric properties provided by HPS
2. A standard gain horn feed from Microwave Vision Group (MVG) described by its measured full sphere pattern provided by Airbus
3. A deployable truss provided by LSS
4. A feed tower provided by HPS

5. Orientation and position of the feed coordinate system and output coordinate system provided by HPS

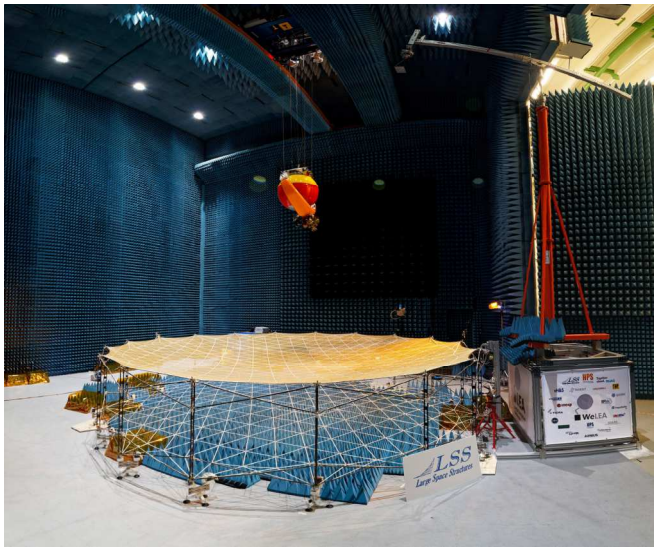

Fig. 1. LEA antenna ready for RF test at Airbus in Ottobrunn, Germany. The crane-based gondola probe of the PAMS system is visible in orange, red and yellow.

The output coordinate system is shown at the bottom left in Fig. 2: it has its z-axis depicted in blue and aligned to the boresight of the antenna, x-axis shown in red and y-axis shown in green. The xz plane of the output coordinate system is called H-pol plane in this paper, and the yz plane of the output coordinate system is called V-pol plane. The measured and the predicted RF patterns refer both to the output coordinate system shown in Fig. 2.

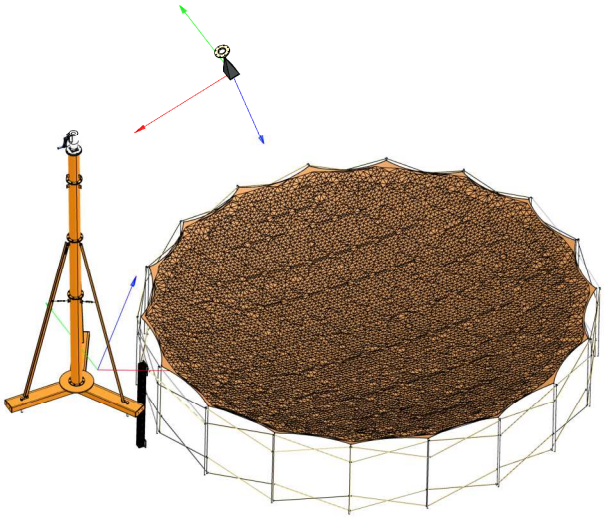

Fig. 2. TICRA Tools RF model of the LEA antenna in RF measurement conditions.

The LEA reflector is illuminated by the SGH820 feed from MVG, which is a single polarized standard gain horn working in the [8.20-12.40] GHz band. The pattern of the feed horn was measured on a full sphere in a far-field facility at Airbus and then provided to TICRA and used as feed in the LEA RF predictions. The same set of measured data was used for both H- and V-Pol, with the feed coordinate system being rotated 90° for V-pol with respect to H-pol. At $\theta$ = 27°, corresponding approximately to the reflector edge, the feed taper relative to peak is around (-26 dB, -16 dB) in the $\varphi$ = (0°, 90°) planes. The feed spill-over is 0.22 dB, corresponding to 95 % of the feed power hitting the reflector.

The LEA reflector surface is constituted by surface points in xyz coordinates, acquired by HPS with a laser radar measurement of the reflector in deployed configuration supported by gravity compensation devices. In addition, extra points on the front tension net were obtained by linearly extrapolating the surfaces of the two adjacent triangles to the nominal net xy coordinates and by averaging the resulting z values. A total of 9179 surface points was considered and linear interpolation was used in between them.

The LEA tricot mesh is made by gold plated tungsten wires with 30 micron diameter. The mesh has the Atlas-Atlas pattern shown in Fig. 3, where the blue grid is 5 mm x 5 mm in width and height. The measured reflection loss at 10.65 GHz for normal incidence and for an x- and y-polarized field were Ry= -0.01 dB and Rx= -0.1 dB, respectively. The rectangular wire mesh model from the GRASP SW was used by TICRA to model the properties of the tricot mesh in the RF analyses. The spacing along the x- and y-direction of the rectangular wire mesh model in GRASP is determined from the reflection loss values measured for normal incidence for the real tricot mesh. Once this is done, the reflection and transmission properties of the rectangular wire mesh model are computed by GRASP with the formulas from Astrakhan [8], for any incidence angle. It is noted that ohmic losses are not included in the GRASP wire mesh model, while transmission and reflection losses are.

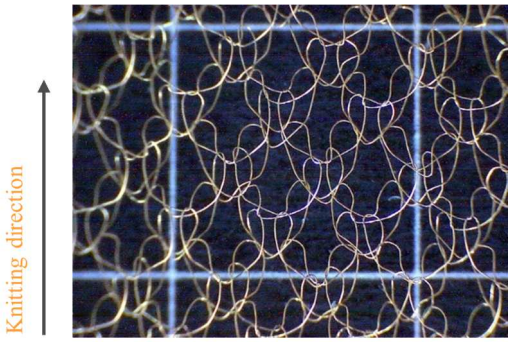


Fig. 3. Sample of the Atlas-Atlas tricot mesh used in the LEA antenna.

To evaluate which analysis method should be used in the RF predictions, the pattern obtained by Physical Optics (PO) for the LEA reflector and feed was compared with the pattern given by a full wave MoM/MLFMM simulation. In the MoM/MLFMM analysis the entire antenna consisting of the LEA reflector, the truss, the feed tower and the feed were simulated and the mutual interaction between the structures

was included. This was done to assess the impact on the antenna pattern from other parts of the structure than the reflector itself. It was seen that the two sets of curves agreed extremely well, and only minor differences were observed at levels below 50 dB from the peak. On this ground, it was concluded that the PO analysis of the feed and reflector was sufficient to accurately predict the LEA antenna patterns, and the feed tower and the truss could thus be disregarded.

## III. Antenna Radiation Patterns

### A. Measured Antenna Patterns

During the RF measurement test in Ottobrunn, the LEA reflector was supported by gravity compensation devices and pointed towards the ceiling. The near-field was measured at 10.4 GHz, 10.65 GHz and 11 GHz for both a H-pol and V-pol feed, on a scan plane of 7 m x 5.5 m normal to the antenna boresight and at a distance of 4.5 m from the center of the reflector surface. The measured near-field was then transformed to a far-field pattern in the range $-20^\circ < \theta < 20^\circ$. The uncertainty of the measured patterns was estimated to be ±0.4 dB on the peak gain and ±5 dB at -30 dB from the peak. The amplitude of the co-polar component of the measured electric field at 10.65 GHz, in Ludwig 3rd polarization for the H-pol feed and in uv coordinates is shown in Fig. 4. The plot shows a well-defined main beam with peak at u=v=0 and the typical grating lobes due to the periodicity of the triangular front tension net.

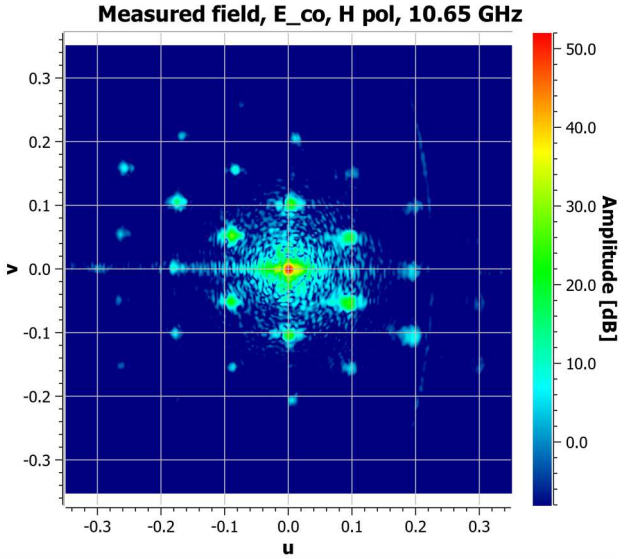


Fig. 4. Amplitude of the co-polar component of the measured electric field at 10.65 GHz, in Ludwig 3rd polarization for the H-pol feed.

### B. Correlation between Measurements and Simulations

The amplitude of the co-polar component of the electric field in Ludwig 3rd polarization at 10.65 GHz, for the H-pol feed and predicted by TICRA with the RF model described in Section II is shown in Fig. 5.

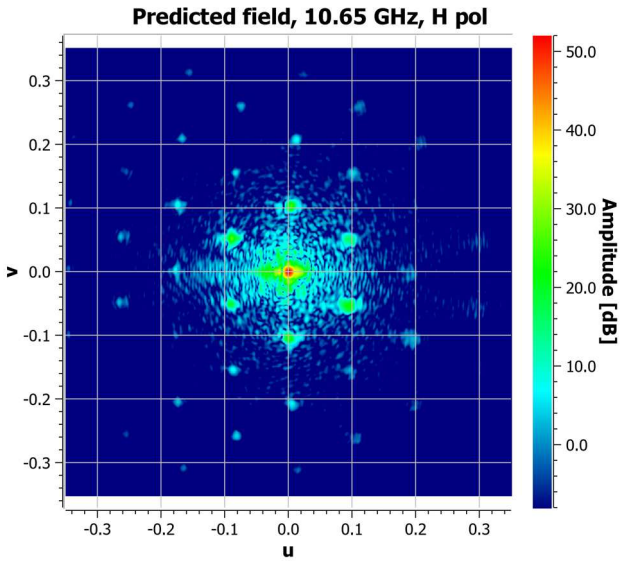


Fig. 5. Amplitude of the co-polar component of the predicted electric field at 10.65 GHz, in Ludwig 3rd polarization for the H-pol feed.

A plot of the measured and predicted co-polar and cross-polar components of the electric field on the two principal cuts is shown in Fig. 6 and Fig. 7 for the H-pol feed at 10.65 GHz, and in Fig. 8 and Fig. 9 for the V-pol feed at 11 GHz. Equivalent plots can be made at 10.4 GHz.

Finally, the amplitude of the predicted co-polar component of the electric field obtained neglecting the reflector surface points extrapolated on the front tension net is shown in Fig. 10. By comparing it with Fig. 5 and Fig. 4, it is clear that in Fig. 10 only the first ring of grating lobes can correctly be predicted and all remaining measured grating lobes are missing.

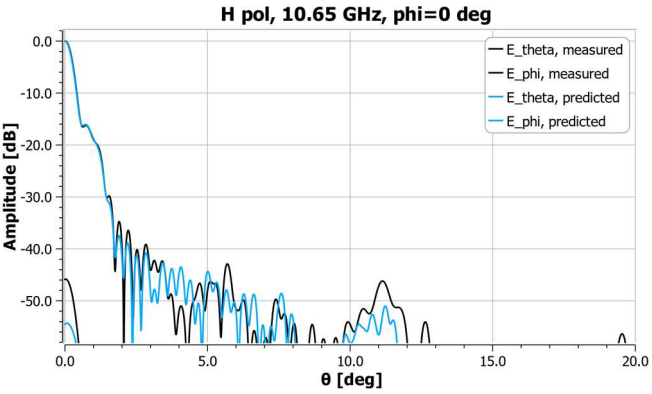


Fig. 6. Amplitude of the co- and cross-polar component of the measured and predicted electric field at 10.65 GHz, in Ludwig 3rd polarization for the H-pol feed and the phi=0 deg plane.

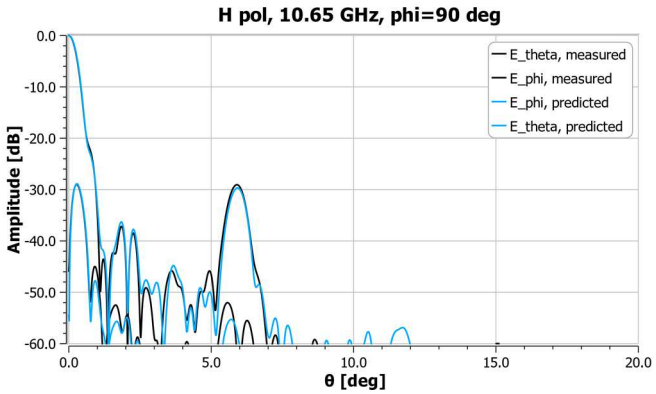


Fig. 7. Amplitude of the co- and cross-polar component of the measured and predicted electric field at 10.65 GHz, in Ludwig 3rd polarization for the H-pol feed and the phi=90 deg plane.

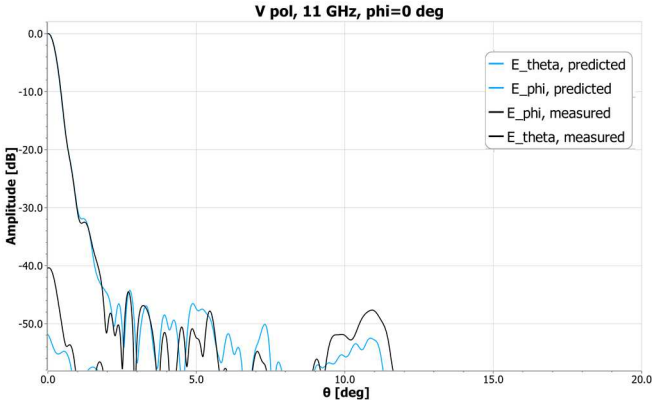


Fig. 8. Amplitude of the co- and cross-polar component of the measured and predicted electric field at 11 GHz, in Ludwig 3rd polarization for the V-pol feed and the phi=0 deg plane.

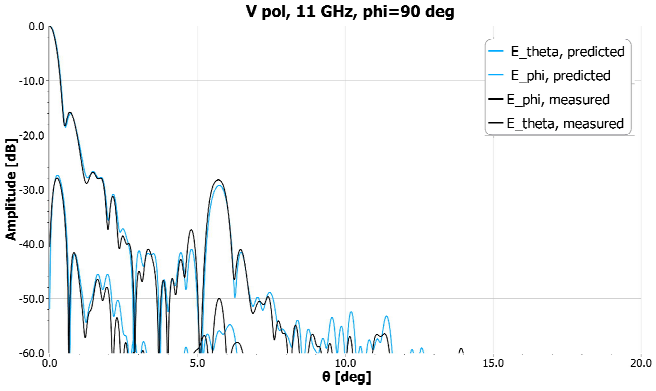


Fig. 9. Amplitude of the co- and cross-polar component of the measured and predicted electric field at 11 GHz, in Ludwig 3rd polarization for the V-pol feed and the phi=90 deg plane.

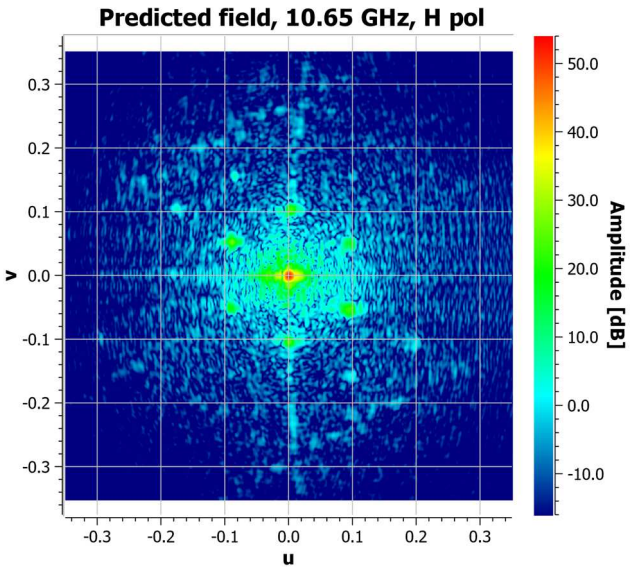


Fig. 10. Amplitude of the co-polar component of the predicted electric field at 10.65 GHz, in Ludwig 3rd polarization for the H-pol feed, when the surface points extrapolated on the front tension net are disregarded.

TABLE I. shows the measured and predicted gain values at all frequencies and for both feed polarizations.

TABLE I. MEASURED AND PREDICTED GAIN VALUES.

| Feed orientation | Frequency [GHz] | Measured gain [dB] | Predicted gain [dB] |
|---|---|---|---|
| **H-pol** | 10.4 | 51.57 | 51.77 |
| **H-pol** | 10.65 | 51.64 | 51.90 |
| **H-pol** | 11.0 | 51.95 | 52.21 |
| **V-pol** | 10.4 | 51.25 | 51.66 |
| **V-pol** | 10.65 | 51.50 | 51.80 |
| **V-pol** | 11.0 | 51.61 | 52.08 |

## IV. CONCLUSIONS

From the RF test correlation exercise described in Section IIIB the following can be concluded.

It is observed that the accurate knowledge of the reflector surface on the front tension net is of fundamental importance for the correct modelling of all grating lobes in amplitude and position. If the surface on the front tension net is not accurately known, only the first ring of grating lobes can be predicted. The reflector surface is currently modelled by combining surface measured points and extrapolated points, to recover the surface information on the front tension net, which was missing from the surface measurement activity.

From the results presented in this paper, this seems to be a good approach.

The agreement between measured and predicted radiation patterns is excellent in the main beam, sidelobes, nulls and grating lobes down to -40 dB from the peak. This is true at all frequencies and for both polarizations of the feed.

The agreement between measured and predicted gain is good. The gain for the H-pol feed is approximately 0.1 dB higher than the value for the V-pol feed. This agrees with the tricot mesh measured reflection losses and the orientation of the tricot mesh relative to the reflector.

The differences between measured and predicted amplitude pattern levels and gain values are well within the estimated measurement uncertainty.

Valuable experience is gained for future measurements and simulations of large deployable reflectors and the correlation between RF measured and predicted patterns is considered successful.

## REFERENCES


[1] https://www.l3harris.com/all-capabilities/unfurlable-mesh-reflector-antennas

[2] https://www.northropgrumman.com/space/astro-aerospace-products-astromesh/

[3] Large European Antenna, http://www.welea.eu/.

[4] L. Datashvili, N. Maghaldadze, M. Friemel, T. Luo, L. da Rocha-Schmidt, C. Cappellin, J. R. de Lasson, R. Jørgensen, J.-C. Angevain, A. Ihle, and L. S. Drioli, “Large deployable reflectors: Enhancing the mesh reflector RF performances,” in 3rd International Conference ”Advanced Lightweight Structures and Reflector Antennas”, September 2018.

[5] J. R. de Lasson, C. Cappellin, R. Jørgensen, L. Datashvili, and J.-C. Angevain, “Advanced techniques for grating lobe reduction for large deployable mesh reflector antennas,” in Antennas and Propagation Society International Symposium, July 2017.

[6] T. Fritzel, A. Geise, C. Hunscher, M. Paquay, “Large-Scale and Motion-Free Antenna Measurements by an Innovative Crane-Aided Near-Field Measurement System (PAMS)”, 37th ESA Antenna Workshop on Large Deployable Antennas, November, 2016.

[7] GRASP and ESTEAM software, TICRA, Denmark, www.ticra.com.

[8] Astrakhan M. I. “Reflecting and screening properties of plane wire grids”, Radio Engineering, Vol. 23, No.1, 1968.